Investigation of Solidification in the Laser Engineered Net Shaping (LENS^{TM}) Process

William Hofmeister and Melissa Wert, Vanderbilt University
John Smugeresky, Joel A. Philliber, Michelle Griffith, and Mark Ensz
Sandia National Laboratories, Albuquerque, NM and Livermore, CA.

The Laser Engineered Net Shaping (LENS^{TM}) process is a laser assisted, direct metal manufacturing process under development at Sandia National Laboratories. The process incorporates features from stereo lithography and laser surfacing, using CAD file cross-sections to control the forming process. Powder metal particles (less than 150 micrometers) are delivered in a gas stream into the focus of a Nd:YAG laser to form a molten pool. The part is then driven on an x/y stage to generate a three-dimensional part by layer wise, additive processing. In an effort to understand the thermal behavior of the LENS process, in-situ high-speed thermal imaging has been coupled with microstructural analysis and finite element modeling. Cooling of the melt is accomplished primarily by conduction of heat through the part and substrate, and depending on the substrate temperature and laser input energy, cooling rates can be varied from 10^2 to 10^3 K s^{-1}. This flexibility allows control of the microstructure and properties in the part. The experiments reported herein were conducted on 316 stainless steel, using two different particle size distributions with two different average particle sizes. Thermal images of the molten pool were analyzed to determine temperature gradients and cooling rates in the vicinity of the molten pool, and this information was correlated to the microstructure and properties of the part. Some preliminary finite element modeling of the LENS process is also presented.

Sandia is a multiprogram laboratory operated by Sandia Corporation, a Lockheed Martin Company, for the U.S. Department of Energy under contract number DE-AC04-94AL85000.

Introduction

Rapid prototyping using the stereo lithography process and plastic materials has enjoyed great success. The natural extension of this process to structural materials has been accomplished with the Selective Laser Sintering (SLS) process. In addition, various methods of laser cladding and laser assisted surface modification are also being practiced. Laser Engineered Net Shaping (LENS^{TM}) builds on SLS process with a few notable exceptions. Instead of bonding material in a bed of powder, the powder is delivered in a gas jet through nozzles. Solid material is formed by solidification of a molten pool, thus forming a fully dense, free standing deposit. LENS development is the subject of a Cooperative Research and Development Activity (CRADA) at Sandia National Laboratory. This technology is being commercialized by several of the CRADA participants.[1]

A photograph of a single pass line build of 316 stainless steel is shown in figure one. The LENS powder delivery system consists of a commercial powder feeder that delivers powder into a gas delivery system by way of the four nozzles shown in the figure. The Nd:YAG laser beam is delivered along the z-axis in the center of the nozzle array and focused by a lens in close proximity to the work piece. The work piece is driven in the x and y directions by a motorized stage. Moving the lens and powder nozzles in the z direction controls the height of the laser and powder focus.

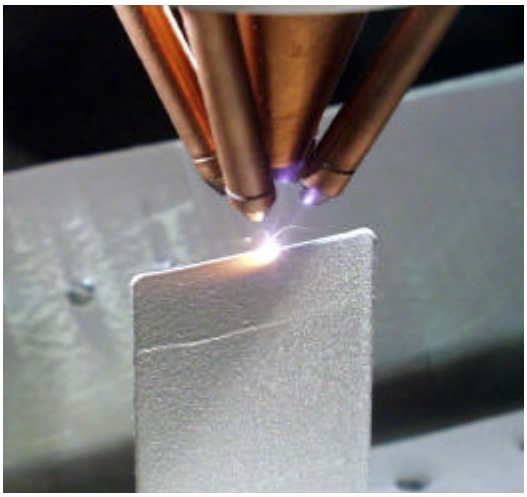

Figure 1: Photograph of the LENS process performing a single line build.

In order to understand the development of structure and properties in the solidified material, it is important to know the thermal gradients and cooling rates in and around the molten pool. These gradients control the morphology and scale of the first solid to form, and are a primary factor in determining the properties of the sample. Since the heat from the melt pool is conducted primarily through the substrate, this thermal information can be used as a boundary condition in heat transfer models to determine the complete thermal history of the sample.

Thermal measurements, microstructural studies, and modeling can be combined to develop process parameters to control microstructural development and tailor the properties of samples for particular applications. As a first step, thermal imaging was employed in monitoring line builds of 316 stainless steel at a variety of laser powers for −100 mesh powder and +100-325 mesh powder. The microstructures of the deposits were investigated and correlated to the thermal conditions at solidification. Finally, a finite element model of the line build process was developed to determine the thermal history of the sample in areas that are not accessible to thermal imaging measurements.

[1] Optomec Design Company, MTS Systems Inc. , AeroMet Corp.

Thermal Imaging

High-speed thermal imaging has been used in the study of solidification kinetics and droplet impact and spreading[2]. For the LENS studies a digital 64x64 pixel CCD video camera was employed. This camera digitizes monochrome images to 12-bits and passes the frame data to a personal computer for storage and processing. A telephoto lens and broad band-pass filter centered at 650 nm were used in the image path. The camera, lens, and filter were calibrated for temperature measurement with a tungsten strip lamp radiance source obtained from the National Institute of Standards and Technology. The experimental setup is shown in figure 2. The powder and laser focus do not move in the x-y plane so that the build could be tracked by adjusting the tilt of the camera. The camera angle was measured with a clinometer and was adjusted as the build progressed. Images were taken at up to 990 frames per second. At the end of each set of imaging experiments, a molten pool was formed with no translation of the work piece to observe the freezing plateau for *in situ* calibration.

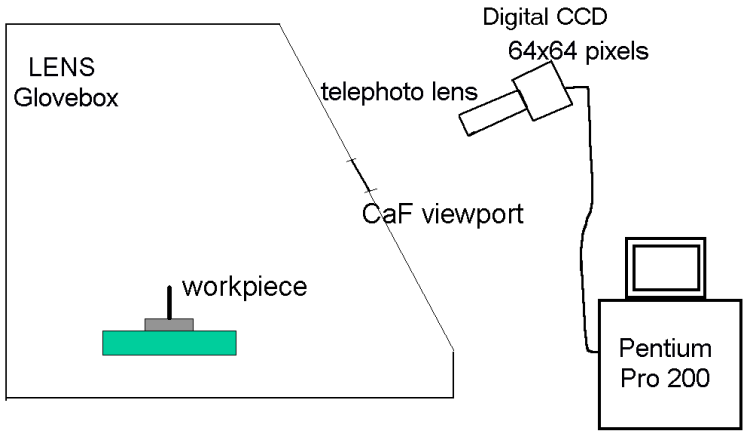

Figure 2: Schematic of thermal imaging experimental setup. The thermal imaging camera views the sample through a CaF viewport in the front of the LENS glovebox.

A typical side view image of a line build is shown in figure 3. The image has been converted to temperature and colorized according to the adjacent scale. The angle of the image to the x-y plane is approximately 30° so that the top surface as well as the front face of the build is visible. Since the angle of the plane of the camera to the sample is known, the distances and temperatures can be corrected for the angle of view. Clicking the following linked object will play a movie of the build.

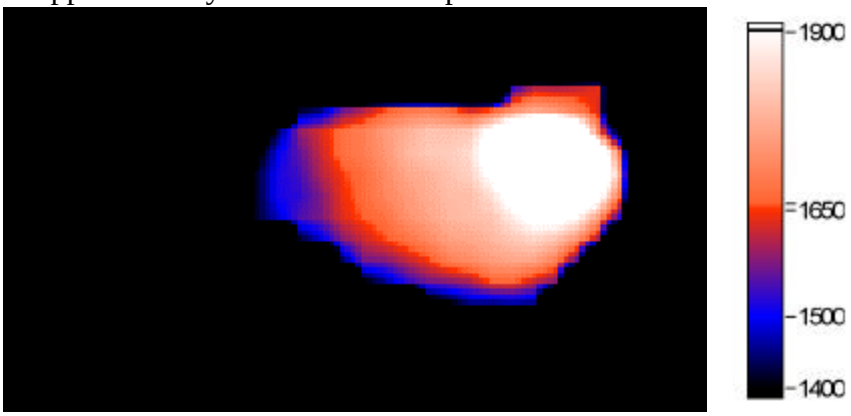

Figure 3: Side view of a LENS line build. The image has been colorized to show temperature in Kelvin.

[2] http://www.vuse.vanderbilt.edu/~aesinfo/mse/dropl.htm

Images of the kind shown in figure 3 were analyzed to determine the isotherms on the side wall of the build. The information from several frames is presented in figure 4 with each frame represented by a different color. The melt isotherm has a length of 0.75 mm.

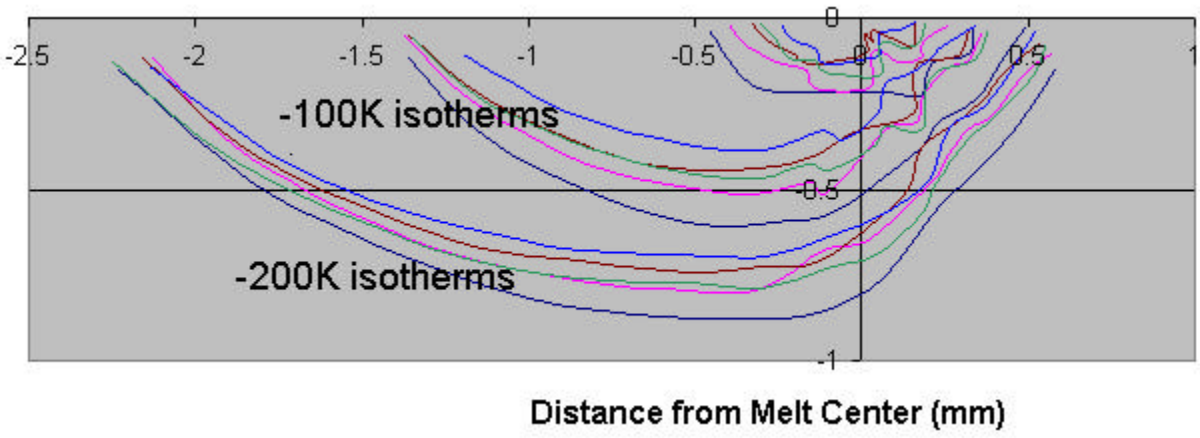

Figure 4: Isotherms at 100K and 200K below the melt on the side wall of a line build are shown in the figure. Each color corresponds to a different image frame of data. The coordinates of the laser spot are (0,0) and the sample is moving from right to left.

The gradients in the previous build layer below the laser are as high as 400K mm^{-1} and taper off to less than 200K mm^{-1} in the trail of the molten pool.

Since the sample is moving in the x-direction, it is possible to scale these gradients with the sample velocity to derive cooling rates for material deposited in the x-direction. For example, in figure 5 the image is shown at the top, and the temperature along the yellow cursor line from the "begin" mark and to the left of that mark is shown in the first graph under the picture. This temperature graph shows the temperature distribution along the direction of travel. This sample was built at a traverse velocity of 7.62 mm s^{-1}, so that the resulting cooling rate can be calculated (dT/dx*dx/dt) and is displayed in the bottom graph of the figure. The highest cooling rates are in the liquid ahead of the solid-liquid interface. At the melting temperature and below, the cooling rates approach 10^3 K s^{-1}.

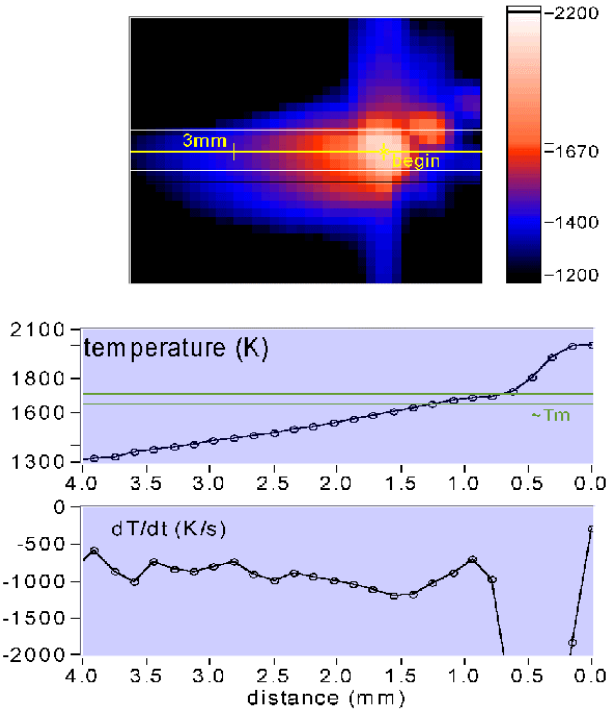

Figure 5: The temperature distribution along the yellow cursor in the thermal image is shown in the temperature graph, and the cooling rate is displayed in the bottom graph.

The thermal profiles of the build reveal interesting nonlinearities in the build process. Profiles similar to those in figure 5 were compiled for line builds as a function of laser power. These are presented in figure 6 for the -100/+325 mesh powder. The laser power for each profile is shown in the legend. The molten pool size increases with power up to 275W. Above 275W the energy of the laser drives the pool temperature up without significant change in the length of the molten zone. Note also that the slopes of the temperature profiles outside the molten zone generally increase as the power decreases. Higher power results in more bulk heating of the sample away from the molten zone. This results in a lower cooling rate in the solid sample after solidification. For example, the cooling rate of the 275W sample 0.5 mm from the solid-liquid interface is twice that of the 410W sample. The initial scale of the microstructure, however, should be determined by the cooling rate at the solid-liquid interface.

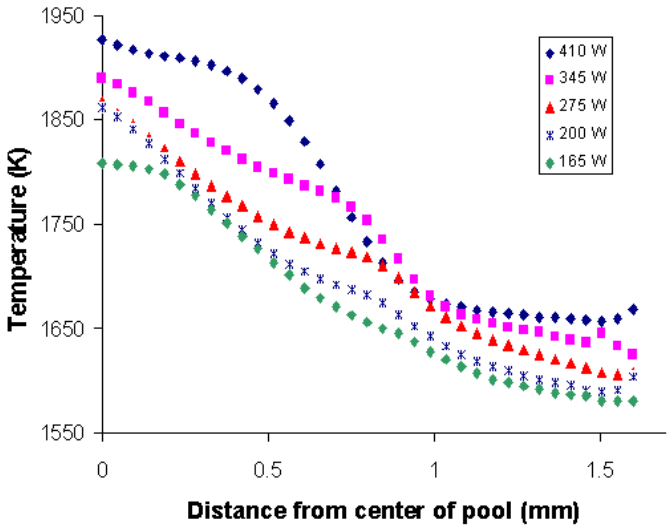

Figure 6: Thermal profiles from the center of the molten pool along the direction of translation for several different laser power settings.

A complete series of line builds was analyzed to determine the cooling rate at the solid-liquid interface. These determinations are shown in figure 7. At the interface the cooling rates are substantially higher at the low power levels and remain fairly constant at the higher powers. Thus, the highest quench rates are available at the lowest power, when the molten zone is small. As the laser power is increased, the quench rate at the interface settles at 1000-1500 K s^{-1}. In the solid, however, the cooling rate at the highest powers is lower so that one may expect a more coarsened microstructure due to grain growth.

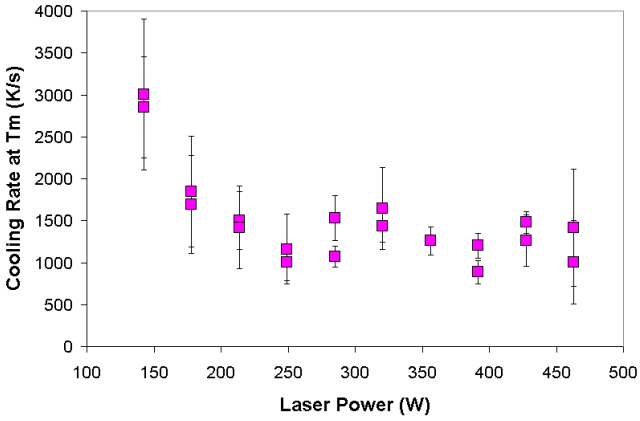

Figure 7: Cooling rates calculated from a large series of images as a function of laser power.

Microstructures

The solidification microstructures of LENS processed 316 stainless steel are complex and varied as one might expect in a rapid solidification structure. In general, near the interface of the molten pool, columnar structures predominate. This feature is clearly seen in the series of microstructures presented in figures 8-13. The remaining regions of the samples have a cellular structure. The

micrographs are montages of optical micrographs taken from a cross section of the samples processed with the -100/+325 mesh powder. The z direction or height of the build is vertical in the micrographs, and the width of the micrographs is the y direction. An oxalic acid electrolytic etch was used to delineate the austenite cell boundaries.


Figure 8: 115 W


Figure 9: 165W


Figure 10: 200W


Figure 11: 275W


Figure 12: 345W


Figure 13: 410W

The dendrites and cells at the lower power levels are finer. At the higher powers significant dendrite coring and cell substructure can be seen. A comparison of the microstructural scale of these samples was obtained by measuring the mean intercept length of cell boundaries with a Hillard circle. These results are presented in the following table. The uncertainty of these determinations is about 10%.

Table 1: Mean intercept length between cell boundaries for +100/-325 mesh powder.

Laser Power (W)	Mean intercept length (microns)
410	8.68
345	8.55
275	7.12
200	6.46
165	4.63
115	3.25

Finite Element Modeling

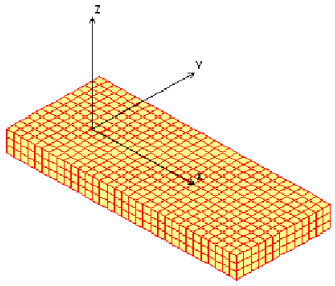

Figure 14: FEA model of the substrate.

The macro-thermal characteristics during part fabrication are important particularly as they apply to solid state transformations, dimensional accuracy and residual stress in built components. Initial work has focused on finite element analysis (FEA) methods with element birthing to simulate LENS processing. The thermal behavior during fabrication of a thin wall has been modeled. The material properties were based on generic stainless steel, and for the initial studies only conduction is used for thermal transfer. The substrate (shown in figure 14) is held at 300° C throughout the simulation, whereas thermocouple data indicates that the substrate

reaches this steady state when the build is approximately 6.3 mm tall. The wall was made of 1.27 mm^3 elements for a 25.4 mm long, 76.2 mm tall wall.

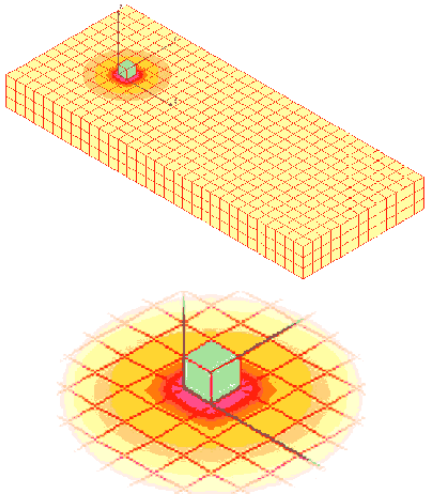

Figure 15: This shows the thermal distribution after the placement of the first element on the substrate.

The first element (shown in figure 15) was positioned onto the substrate with a set initial temperature at all of the eight nodes. These nodes were set at the melting temperature (1377^{o}C) for one set of FEA experiments, and at a superheat temperature (1627^{o}C) for another set following the results of the imaging experiments. The element was held at the set temperature for the amount of time the laser dwells at this position, and then the model computed the final temperature values or nodes in the model (element plus substrate) and stored the data.

For subsequent elements (figure 16), the model used the results from the previous step as the initial condition for each new element birth. Once again, the new element was set at the initial temperature, the time step was calculated and the temperature data for all elements stored. This was repeated for all birthing events until the geometry was complete. The entire simulation of the wall build has been assembled in the form of a movie. As seen in the movie, large thermal gradients exist in the LENS process. Near the molten pool, the energy is concentrated, and the thermal gradients are steep. Far from the molten pool, the gradients reach a steady-state thermal front, where the base is the main conduction path for the energy. A clear picture of LENS thermal behavior can be obtained by understanding these gradients and refining the model with experimental verification.

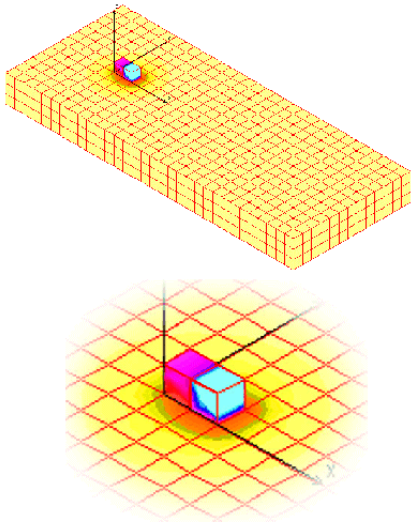

Figure 16: The thermal distribution after addition of the second element.

Meshing algorithms are being developed to decrease the processing time per element birth sequence in order to utilize these techniques for complex components. FEA will be used to determine where the thermal gradients exist, especially with respect to complex part geometry to reduce distortion and thermal stresses in part fabrication. Furthermore, understanding the thermal behavior will clarify the microstructural effects of these gradients on final properties for LENS fabricated components.